MODELING AND CONTROL OF A VISCOELASTIC PIEZOLAMINATED BEAM

Peter Nauclér [*] **Hans Norlander** [*] **Anders Jansson** [**]
Torsten Söderström [*]

[*] *Division of Systems and Control, Department of Information Technology, Uppsala University*
P O Box 337, SE-75105 Uppsala, Sweden
[**] *Solid Mechanics, Department of Engineering Sciences, Uppsala University*

Abstract: Modeling and control of a viscoelastic beam are considered. Piezoelectrical elements are bonded to the beam and used as actuators. The beam is also equipped with a strain gauge that serves as a sensing device. The beam system is described by the Euler-Bernoulli beam equation, which is Fourier transformed and numerically solved in the frequency domain. Then, two different approaches are evaluated to approximate the infinite-dimensional system with a low order parametric approximation. Finally, LQG control theory is applied to control both strain and transversal vibrations. Especially, the control of the strain shows promising results.

Keywords: Mechanical systems; vibration control; LQG control; smart structures; frequency response data

1. INTRODUCTION

The presence of vibrations is a common problem in mechanical structures, particularly in flexible parts, for instance aircraft wings or robot arms. This can be reduced by making such parts strong or heavy enough. For many applications, *e.g.* in aircrafts and spacecrafts, it is desirable to keep the weight as low as possible, which makes such solutions less suitable. Instead, one would like to have a device which can perform active damping of the vibrations without any substantial increase of the mass. In the case when such a device is embedded in the structure it is often referred to as a smart material or a smart structure (Preumont, 2002).

One way to design smart structures is to use piezoelectric elements that are attached to the material. Piezoelectric elements exhibit a significant deformation when an electric field is applied, and they produce an electric field when deformed. Therefore they can be used as both actuators and sensors in a smart structure. Using piezoelectric patches is a simple and cheap way of integrating actuating and sensing devices in mechanical structures. Modeling and control of simple flexible structures have received a lot of attention in recent years; see for example (Pota and Alberts, 1995), (Moheimani *et al.*, 2003) and the references therein.

A popular setup is to use a steel beam that is simply supported at both ends. Often the beam is equipped with collocated piezoelectric actuator-sensor pairs which conveys that the tractable passivity property can be used for controller design. This is utilized in (Halim and Moheimani, 2001), which employs the popular modal analysis technique, or assumed modes approach, for describing the dynamics of the system. In this method the orthogonality between vibration modes is used to obtain transfer functions which have the form of infinite sums; each term describing one vibrational mode. The sum is then truncated to obtain

a low order approximation of the infinite-dimensional system.

There are, however, a number of disadvantages related to the modal analysis technique. First of all the method assumes pure elasticity which means that no damping is present. This is most often compensated for by adding a small damping term to each vibrational mode in an ad-hoc manner. In addition, the piezoelectric sensor/actuator is assumed not to affect the structural properties of the beam. To take the piezoelectrical patches into account the system gets a more complex structure and the modal analysis technique can no longer be applied.

In this paper we present a procedure for how to model a viscoelastic beam structure where the piezoelements are taken into account. Furthermore, damping is included in the modeling phase by using a complex valued Young's modulus which was experimentally determined in (Hillström *et al.*, 2003). Piezoelectrical patches are bonded to each side of the beam and used as actuators. As a sensing device a strain gauge is attached to the beam. It consists of a thin wire whose effect on the structural properties of the beam is negligible.

2. PROBLEM FORMULATION

Consider an experimental setup as in Figure 1. A viscoelastic beam is fixed at one end and free at the other. The beam is divided into three sections and piezoelectric patches are attached to the beam at its middle section. A disturbance force $f(t)$ enters at the tip of the beam, possibly as an impulse. The beam is also equipped with one sensor that measures the strain, $y(t) = \varepsilon(t, \xi)$, at a spatial position ξ, that arises due to the impact of $f(t)$. The measured signal is corrupted with additive noise, $e(t)$.

Our goal is to dampen the vibrations in the beam by applying a controller that uses the strain measurements in a feedback loop. The control signal $u(t)$ is fed to the piezoelectric patches which are used as actuators. The system can be schematically described as in the lower part of Figure 1. By using the properties of linear systems, the output signal can be viewed as a superposition of the strains caused by $u(t)$ and $f(t)$. The control signal affects the output through the transfer function $G(s)$, and the force contributes through the transfer function $H(s)$.

The vibrations in the beam are mathematically described by a partial differential equation (PDE), which means that the system is of infinite order. The piezoelectric patches are considerably stiffer than the rest of the beam. This is a fact that is accounted for in the modeling. The strain sensor is, however, very small and of negligible weight. It should thus not contribute to the dynamics of the system. We aim at describing the infinite dimensional system with a parametric

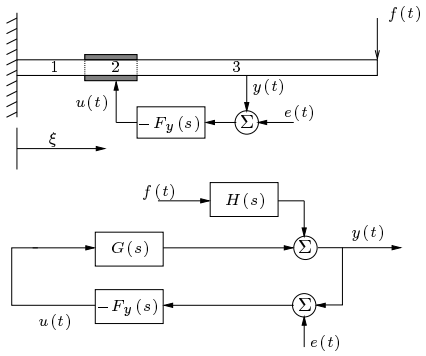

Fig. 1. An experimental setup of a viscoelastic beam with piezoelectric patches (actuator) and a strain sensor.

Table 1. Properties of the beam and the piezoelement.

Description	Value
Beam length [m]	0.59
Beam width [m]	0.01
Beam thickness [m]	0.002
Beam density [kg/m^3]	1183
Piezo. length [m]	0.0318
Piezo. thickness [m]	0.00066
Piezo. density [kg/m^3]	7878
Piezo. Young's modulus [N/m^2]	5.78×10^{10}
Length of first section [m]	0.202

model of finite order. This model should then be a basis for model-based control. The properties of the beam are listed in Table 1.

3. MODELING

Although the strain is measured, we first consider modeling of the transversal deflection, w, at each section, k, of an *elastic* beam. At a spatial coordinate ξ at time instance t the deviation can be described by the PDE

$$\frac{\partial^2}{\partial \xi^2}\Big[E_k I_k \frac{\partial^2 w_k(t,\xi)}{\partial \xi^2}\Big] + \rho_k A_k \frac{\partial^2 w_k(t,\xi)}{\partial t^2} = 0 \quad (1)$$

which is called the Euler-Bernoulli beam equation (Timoshenko, 1955). The quantities I_k, A_k and ρ_k represent the moment of inertia of a cross-section area, cross-section area and density, respectively. These parameters are assumed to be time invariant and spatially constant for each section, k, of the beam. The Young's modulus of elasticity is denoted by E_k. In the pure elastic case, this quantity is constant and real-valued for each section of the beam. By Fourier transformation of (1) w.r.t. the temporal variable, the PDE is transformed to a frequency dependent ordinary differential equation in the spatial domain, ξ

$$E_k I_k \frac{\mathrm{d}^4 W_k^{\mathcal{F}}(\omega,\xi)}{\mathrm{d}\xi^4} - \rho_k A_k \omega^2 W_k^{\mathcal{F}}(\omega,\xi) = 0 \quad (2)$$

where $W_k^{\mathcal{F}}(\omega,\xi)$ is the Fourier transform of $w_k(t,\xi)$ and ω is the angular frequency [rad/s]. In the sequel we will deal with both the Fourier transform and the Laplace transform. To separate the two transforms

the superscripts $\mathcal{F}$ (Fourier) and $\mathcal{L}$ (Laplace) will be employed.

A *viscoelastic* beam exhibit the property that if the deformation is specified, the current stress depends on the entire deformation history. This is described by a Young's modulus that is frequency dependent and complex valued (Christensen, 1971). Based on this, viscoelasticity can be introduced in a frequency domain context by replacing E_k in (2) with $E_k(\omega)$. The frequency dependent Young's modulus was experimentally determined in (Hillström *et al.*, 2003). To solve (2) a number of boundary values and compatibility conditions are needed. The (Fourier transformed) boundary values of the cantilever beam are

$$W_1^{\mathcal{F}}(\omega,0) = \mathbf{D}W_1^{\mathcal{F}}(\omega,0) = \mathbf{D}^2 W_3^{\mathcal{F}}(\omega,L) = 0$$
$$E_3(\omega) I_3 \mathbf{D}^3 W_3^{\mathcal{F}}(\omega,L) = F^{\mathcal{F}}(\omega)$$

where $\mathbf{D} = \frac{\mathrm{d}}{\mathrm{d}\xi}$ is the differentiation operator. Furthermore the sections of the beam are tied together by four compatibility conditions at each point where two sections meet. For example, if sections k and $k+1$ meet at the spatial coordinate ξ_k the following must hold

$$W_k^{\mathcal{F}}(\omega,\xi_k) = W_{k+1}^{\mathcal{F}}(\omega,\xi_k)$$
$$\mathbf{D}W_k^{\mathcal{F}}(\omega,\xi_k) = \mathbf{D}W_{k+1}^{\mathcal{F}}(\omega,\xi_k)$$
$$M_k^{\mathcal{F}}(\omega,\xi_k) = M_{k+1}^{\mathcal{F}}(\omega,\xi_k)$$
$$T_k^{\mathcal{F}}(\omega,\xi_k) = T_{k+1}^{\mathcal{F}}(\omega,\xi_k)$$

where M and T are the bending moment and transversal force, respectively.

The disturbance force, $F^{\mathcal{F}}(\omega) = \mathcal{F}[f(t)](\omega)$, and the actuating voltage, $U^{\mathcal{F}}(\omega) = \mathcal{F}[u(t)](\omega)$, are treated as input signals to the system. $F^{\mathcal{F}}(\omega)$ enters through one of the boundary conditions and $U^{\mathcal{F}}(\omega)$ enters through two of the compatibility conditions.

Using the above observations we replace E_k by $E_k(\omega)$ and solve (2). Its characteristic equation now reads

$$r_k^4 - \omega^2 \frac{\rho_k A_k}{E_k(\omega) I_k} = 0$$

with the solution

$$r_{k,l} = \mathrm{i}^l \left(\omega^2 \frac{\rho_k A_k}{E_k(\omega) I_k} \right)^{\frac{1}{4}}, \quad l = 1,\ldots,4$$

where $\mathrm{i} = \sqrt{-1}$. The solution to (2) is readily written

$$W_k^{\mathcal{F}}(\omega,\xi) = [\mathrm{e}^{\xi r_{k,1}} \ldots \mathrm{e}^{\xi r_{k,4}}][c_{k,1}(\omega) \ldots c_{k,4}(\omega)]^T$$
$$\triangleq \mathbf{R}_k^T(\omega,\xi)\mathbf{C}_k(\omega) \quad (3)$$

where $c_{k,l}(\omega)$ are unknown parameters that are to be determined by using the boundary values and compatibility conditions. Now, denote

$$\mathcal{C}(\omega) \triangleq [\mathbf{C}_1^T(\omega)\ \mathbf{C}_2^T(\omega)\ \mathbf{C}_3^T(\omega)]^T \quad \in \mathbb{R}^{12\times 1}. \quad (4)$$

Then, the following system of equations can be formed

$$\mathcal{A}(\omega)\mathcal{C}(\omega) = \mathcal{B}_1 F^{\mathcal{F}}(\omega) + \mathcal{B}_2 U^{\mathcal{F}}(\omega) \quad (5)$$

where $\mathcal{A}(\omega) \in \mathbb{C}^{12\times 12}$, $\mathcal{B}_1$ and $\mathcal{B}_2 \in \mathbb{R}^{12\times 1}$ are completely determined by the boundary values and compatibility conditions (*i.e.* fully known). The input signals enters through the right hand side of the equation. Using (4) and (5) we have

$$\mathbf{C}_k(\omega) = \mathbf{P}_k \mathcal{A}^{-1}(\omega)\left(\mathcal{B}_1 F^{\mathcal{F}}(\omega) + \mathcal{B}_2 U^{\mathcal{F}}(\omega)\right) \quad (6)$$

where $\mathbf{P}_k \in \mathbb{R}^{4\times 12}$ is constructed such that $\mathbf{P}_k\mathcal{C}(\omega) = \mathbf{C}_k(\omega)$. Finally, combining (6) and (3) the frequency responses from the inputs to the transversal deflection at the coordinate ξ is extracted

$$\begin{aligned} W_k^{\mathcal{F}}(\omega,\xi) &= \mathbf{R}_k^T(\omega,\xi)\mathbf{P}_k\mathcal{A}^{-1}(\omega)\mathcal{B}_1 F^{\mathcal{F}}(\omega) \\ &\quad + \mathbf{R}_k^T(\omega,\xi)\mathbf{P}_k\mathcal{A}^{-1}(\omega)\mathcal{B}_2 U^{\mathcal{F}}(\omega) \\ &\triangleq H_w^{\mathcal{F}}(\omega,\xi)F^{\mathcal{F}}(\omega) + G_w^{\mathcal{F}}(\omega,\xi)U^{\mathcal{F}}(\omega) \quad (7) \end{aligned}$$

The subscript w in the last line of (7) denotes that it is the frequency response to the *transversal deflection* and not the *strain* as in Figure 1. To obtain an expression for the strain, ε_k, as a function of frequency and space, compatibility conditions are utilized (Gere and Timoshenko, 1991)

$$Y^{\mathcal{F}}(\omega) = \varepsilon_k^{\mathcal{F}}(\omega,\xi) = -\frac{h_k}{2}\mathbf{D}^2 W_k^{\mathcal{F}}(\omega,\xi) \quad (8)$$

where h_k is the height of the beam at section k. To find the frequency responses $H^{\mathcal{F}}(\omega,\xi)$ and $G^{\mathcal{F}}(\omega,\xi)$, (8) is simply applied to (7), noting that R_k^T is the only term depending on ξ.

Due to the complexity of $\mathcal{A}(\omega)$ it is not possible to obtain a simple closed form expression directly from the above equations. Instead $H^{\mathcal{F}}(\omega,\xi)$ and $G^{\mathcal{F}}(\omega,\xi)$ can be numerically computed for any frequency or spatial coordinate. Typically, the spatial coordinate is held fixed and the frequency is varied to obtain the frequency responses. Utilizing this, we drop the spatial dependence and introduce the shortened notations $H^{\mathcal{F}}(\omega)$ and $G^{\mathcal{F}}(\omega)$. Solving (7) directly is, however, not numerically sound. Instead, (5) is first solved by means of an LU factorization and the result is put into (3) in a second step. Finally, (8) is applied to get an expression for the strain.

It is most often desirable to have a *parametric* model of finite order that describes the dynamics of a system; not the least if the model should be a basis for model based control. In the following, two different strategies for fitting parametric models to the frequency responses are evaluated.

3.1 An Ad-hoc Approach

The first approach is to realize the transfer functions as proper rational functions in the Laplace domain, *i.e.*

$$\hat{H}^{\mathcal{L}}(s,\theta_H) = \frac{B_H(s)}{A(s)}, \qquad \hat{G}^{\mathcal{L}}(s,\theta_G) = \frac{B_G(s)}{A(s)}$$

where $A(s)$, $B_H(s)$ and $B_G(s)$ are polynomials of order na, nb_H and nb_G, respectively. The parameter vector θ_H contains the coefficients of the unknown polynomials $A(s)$ and $B_H(s)$, *i.e.* $\theta_H = [a_1\ \ldots\ a_{na}\ b_0\ \ldots\ b_{nb_H}]^T$; whereas θ_G only contains

the coefficients of $B_G(s)$. The reason for this convention should soon be clear. To find θ_H we attempt to minimize a quadratic criterion

$$V(\theta_H) = \sum_{k=1}^{N} \left| H^{\mathcal{F}}(\omega_k) - \hat{H}^{\mathcal{L}}(\mathrm{i}\omega_k, \theta_H) \right|^2 W(\omega_k) \tag{9}$$

where N is the number of frequency points at which $H^{\mathcal{F}}(\omega)$ is computed and $W(\omega)$ is a user chosen weighting function. To minimize $V(\theta_H)$ the MATLAB function `invfreqs` is used. It applies a damped Gauss-Newton iterative search algorithm (Ljung, 1988). Once acceptable estimates of $A(s)$ and $B_H(s)$ are obtained, $A(s)$ is used when determining $\hat{G}^{\mathcal{L}}(s, \theta_G) = B_G(s)/A(s)$ in a second step. This is performed by using the same type of loss function as in (9). Since $A(s)$ is now known this will be a linear problem which is solved by using a standard weighted least squares procedure. It is then straightforward to carry on and compute zero-polynomials for any sensor location along the beam, using the pole polynomial from the first identification step.

Example 1. Now, this method is applied to the beam-system in Section 2. A collocated actuator-sensor configuration is used, *i.e.* the sensor is attached on top of one of the actuators. Figure 2 shows the magnitude of the numerically computed $H^{\mathcal{F}}(\omega)$ and its low order approximation $\hat{H}^{\mathcal{L}}(s, \theta_H)$ evaluated on the imaginary axis; *i.e.* $s = \mathrm{i}\omega$. $H^{\mathcal{F}}(\omega)$ is used as frequency domain data for the first identification step. In addition, the magnitude of the error between the two frequency responses is depicted. The thick dash-dotted line denotes an ideal low-pass filter which is used to delimit the part of the frequency response that is utilized for the identification. The rational transfer function $\hat{H}^{\mathcal{L}}(s, \theta)$ has four zeros and six poles, that are fitted to the data set.

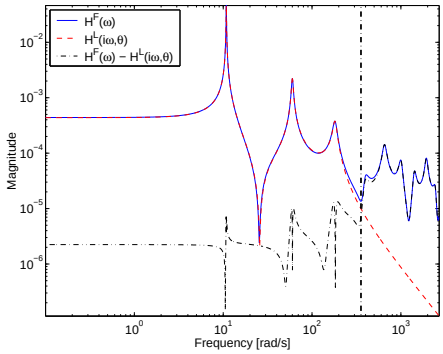

Fig. 2. Magnitude plot of the numerically computed transfer function $H^{\mathcal{F}}(\omega)$ (solid), the low order parametric approximation $\hat{H}^{\mathcal{L}}(\mathrm{i}\omega, \theta)$ (dashed) and the error (dash-dotted).

The figure shows that a very good fit between the frequency response data and the parametric model is obtained. ■

The advantage of this simple method include that frequency weighting is easily performed and that continuous time parametric models are directly obtained. In addition, the method allows arbitrary spacing of the frequency points. It is thus possible to use *e.g.* logarithmically spaced frequency response data to get a natural weighting of the data. Nevertheless, there are some disadvantages. The most obvious one is that only one data set is used to identify the pole polynomial. This could be a real problem if pole-zero cancellation is hidden in the data set chosen for the first identification step. It is also not obvious how to choose model orders and how to realize the system in a state space representation; not the least if a large number of outputs are used. Further, the numerical search procedure in the first identification step is quite expensive computationally.

3.2 Subspace-based Identification

The subspace based algorithm is the algorithm denoted *Algorithm 1* in the paper (McKelvey *et al.*, 1996). It utilizes frequency response data from infinite-dimensional systems to identify MIMO state space models. The frequency response data are restricted to be generated from equidistant frequency samples.

The method is based on estimating the impulse response coefficients by using the inverse discrete Fourier transform on the frequency response data. Then, the coefficients are used to construct a block Hankel matrix on which a singular value decomposition (SVD) is performed. The sub-matrices from the SVD that correspond to the most significant singular values are used to construct the state space representation. In contrast to the ad-hoc approach outlined in the previous section, this method estimates discrete-time models. To convert the models to continuous-time the zero-order hold approach is utilized.

Example 2. Now, the subspace-based approach is applied to find a low order approximation of $H^{\mathcal{F}}(\omega)$ as in Example 1. Once again, the dashed-dotted line denotes an ideal low pass filter which defines the part of the frequency response that is used for the identification. In Figure 3 a state space representation of order six is chosen.

The solid and dashed lines depict that a quite good fit between the parametric model and the frequency response data is obtained. However, the dash-dotted line indicates that the high performance of the ad-hoc approach is not attained. ■

The advantage of this method is that frequency response data from all transfer functions are used to estimate the low order parametric approximation in a single step. The retrieved model is a MIMO state space representation, which is useful for controller design purposes. In addition, the singular values of the Hankel matrix provide a tool for determining the order of the representation. The disadvantage is primarily the lack of a frequency weighting possibility.

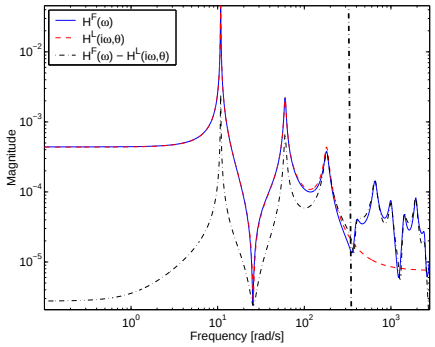

Fig. 3. Magnitude plot of the numerically computed transfer function $H^{\mathcal{F}}(\omega)$ (solid), the low order parametric approximation $\hat{H}^{\mathcal{L}}(\mathrm{i}\omega, \theta)$ (dashed) and the error (dash-dotted). The parametric model is generated from the subspace-based approach.

4. CONTROLLER DESIGN

In order to apply controller design the system is realized in state space form

$$\begin{aligned} \dot{x}(t) &= \mathbf{A}x(t) + \mathbf{B}u(t) + \mathbf{N}f(t) \\ z(t) &= \mathbf{M}x(t) + D_1 u(t) \\ y(t) &= \mathbf{C}x(t) + D_2 u(t) \\ \tilde{y}(t) &= y(t) + e(t) \end{aligned} \tag{10}$$

where $y(t)$, $z(t)$ and $e(t)$ are the strain, transversal deflection and measurement noise, respectively. The unit of the strain is $[1]$ and the unit of the transversal deflection is $[m]$. Although the strain is measured, $z(t) = w(t, \xi)$ is also modeled. The reason for this is that it may be desirable to control the transversal deflection.

This section is divided into two parts. First, LQG-control theory is applied to control the strain. Thereafter, an attempt is made to control the transversal deflection. For simplicity, the subspace-based approach is utilized to model the beam system. This method directly yields a model of the form (10).

4.1 Control of the Strain

For controller design purposes the machinery of LQG control theory is utilized, see *e.g.* (Glad and Ljung, 2000). A controller of the form

$$\begin{aligned} u(t) &= -L\hat{x}(t) \\ \dot{\hat{x}}(t) &= \mathbf{A}\hat{x}(t) + \mathbf{B}u(t) + K(\tilde{y}(t) - C\hat{x}(t) - D_2 u(t)) \end{aligned} \tag{11}$$

is then retrieved.

To find the controller, the following quadratic criterion is employed

$$J = \int_0^\infty [q_y y^2(t) + q_z z^2(t) + u^2(t)]\mathrm{dt} \tag{12}$$

with $q_y = 10^4$ and $q_z = 0$. When determining the Kalman gain, K, the variance of the disturbance, R_1, and the variance of the measurement noise, R_2, are treated as design variables. The values $R_1 = 5 \cdot 10^7$ and $R_2 = 1$ are chosen.

The system is simulated in MATLAB, with a small noise term added to the measured signal. Figure 4 shows the time response, $y(t)$, to an impulse disturbance, $f(t)$. The disturbance is of low-pass characteristics and has its main power within the modeled part of the spectrum. The figure shows that the disturbance

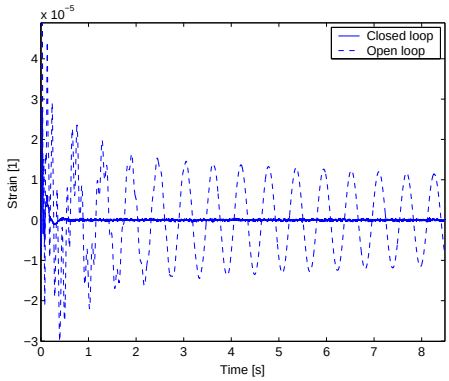

Fig. 4. The time response of the strain. Closed loop (solid) and open loop (dashed).

is well damped if control action is applied. To analyze stability due to unmodeled dynamics the Bode diagram of the loop gain is drawn. Here, the *numerically computed* frequency response $G^{\mathcal{F}}(\omega)$ is employed. It is performed by evaluating the controller (11) for different frequencies and the result is multiplied with $G^{\mathcal{F}}(\omega)$. The Bode plot of the loop gain is depicted in Figure 5. In addition, the sensitivity function, S, and the complementary sensitivity function, T, are visualized in the upper part of the figure.

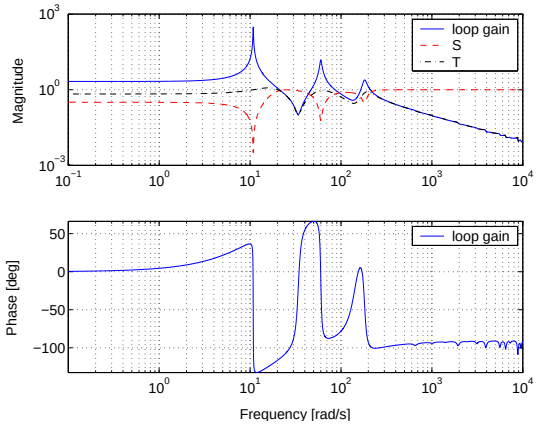

Fig. 5. The Bode plots of the loop gain (solid), S (dashed) and T (dash-dotted).

In view of the figure it should be clear that the closed loop system is robust against the ignored dynamics, since the high frequency content of $G^{\mathcal{F}}(\omega)$ is well damped by the controller. The sensitivity function shows how *sensitive* the closed loop system is to modeling errors. Thus, in frequency regions where S is small the closed loop system is insensitive to

modeling errors. The figure shows that S is quite small in regions where $H^{\mathcal{F}}(\omega)$ is large. Often, one would like to obtain $S(0) \approx 0$ (integral action in the control loop), in order to get rid of stationary errors. However, due to the nature of the disturbance force (impulse), there is no need for integral action in the control loop. The complementary sensitivity also has a reasonable behavior.

4.2 Control of the Transversal Deflection

Now, the transversal deflection, $z(t)$, is controlled. Still, the model (10) is employed, *i.e.* the strain is measured. The parameters $q_y = 0$, $q_z = 1$ and $R_1 = 10^6$ are adjusted. The time response of the transversal deflection is depicted in Figure 6. Once again it is seen

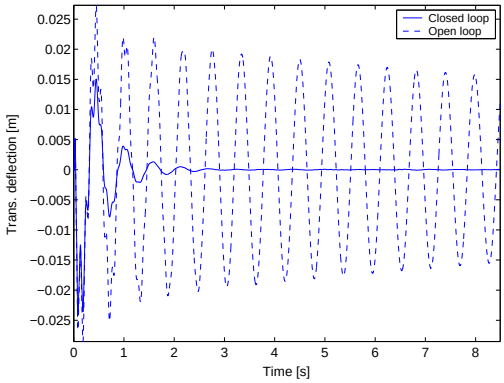

Fig. 6. The time response of the trans. deflection. Closed loop (solid) and open loop (dashed).

that the vibrations are nicely damped when control action is applied. In the same fashion as previously the loop gain, S and T are plotted for the new controller, see Figure 7. The Bode plot of the loop gain shows that

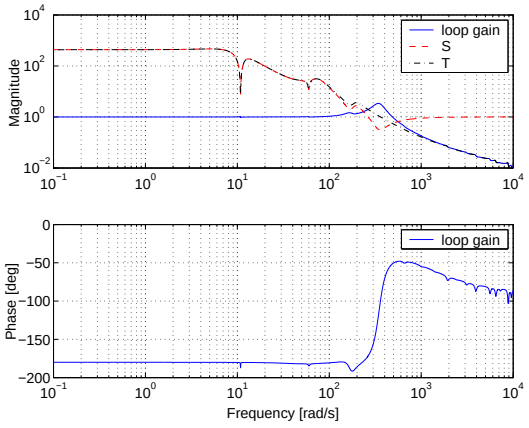

Fig. 7. The Bode plots of the loop gain (solid), S (dashed) and T (dash-dotted). The transversal deflection is controlled.

a very small phase margin is obtained. The sensitivity function and the complementary sensitivity function also have a very unpleasant appearance. The result indicates that it is quite hard to control the transversal deflection from strain measurements.

5. CONCLUSIONS

In this paper, modeling and control of the vibrations in a viscoelastic beam have been considered. For control purposes the beam is equipped with a piezoelectrical actuator and a strain sensor. The aim has been to accurately model the beam system by taking the structural properties of the piezoelectrical actuator into account. In addition, viscoelasticity is introduced in a frequency domain context by employing a frequency dependent Young's modulus of elasticity. The system is described by equations of infinite order and two approaches for model reduction have been treated. Both methods showed nice results.

Finally, LQG control theory was applied to the system. First the strain was controlled with promising result. Then, the transversal deflection was controlled by using the strain measurements in a feedback loop. Even though the vibrations were well damped the Bode plot of the loop gain indicated severe robustness problems.

REFERENCES

Christensen, R.M. (1971). *Theory of Viscoelasticity. An Introduction*. Academic Press. New York, NY.

Gere, J.M. and S.P. Timoshenko (1991). *Mechanics of Materials*. Chapman & Hall. UK.

Glad, T. and L. Ljung (2000). *Control Theory*. Taylor and Francis. UK.

Halim, D. and S.O.R. Moheimani (2001). Spatial resonant control of flexible structures - application to a piezoelectric laminate beam. *IEEE Trans. on Control Systems Technology* **9**(1), 37–53.

Hillström, L., U. Valdek and B. Lundberg (2003). Estimation of the state vector and identification of of the complex modulus of a beam. *Journal of Sound and Vibration* **261**, 653–673.

Ljung, L. (1988). *System Identification Toolbox for use with MATLAB: User's Guide*. The Mathworks. Cochituate Place, 24 Prime Park Way, Natick, MA, USA.

McKelvey, T., H. Akcay and L. Ljung (1996). Subspace-based identification of infinite-dimensional multivariable systems from frequency-response data. *Automatica* **32**(6), 885–902.

Moheimani, S.O.R., D. Halim and A.J. Fleming (2003). *Spatial Control of Vibration: Theory and Experiments*. World Scientific Publishing Co. Pte. Ltd.. Singapore.

Pota, H.R. and T.E. Alberts (1995). Multivariable transfer functions for a slewing piezoelectric laminate beam. *ASME J. of Dyn. Syst., Measurement, Contr.* **117**(3), 352–359.

Preumont, A. (2002). *Vibration Control of Active Structures: An Introduction*. Kluwer Academic Publisher. Dordrecht.

Timoshenko, S. (1955). *Vibration Problems in Engineering*. 3rd ed.. D. Van Nostrand Company. Princeton, NJ.